Nonlinear, dispersive, and phase-matching properties of the new chalcopyrite $CdSiP_2$

Vincent Kemlin,[1] Benoit Boulanger,[1,*] Valentin Petrov,[2] Patricia Segonds,[1] B. Ménaert,[1] Peter G. Schunneman,[3] and Kevin T. Zawilski[3]

[1]*Institut Néel CNRS Université Joseph Fourier, 25 rue des Martyrs, BP 166, 38042 Grenoble Cedex 9, France*
[2]*Max-Born-Institute for Nonlinear Optics and Ultrafast Spectroscopy, 2A Max-Born-Strasse, D-12489 Berlin, Germany*
[3]*BAE Systems, MER15-1813, P.O. Box 868, Nashua, NH 0306, USA*
**benoit.boulanger@grenoble.cnrs.fr*

Abstract: We compare the nonlinear and dispersive properties of the recently discovered mid-infrared nonlinear crystal $CdSiP_2$ with other chalcopyrite materials to establish its potential for super-continuum generation through a second-order nonlinear process.

OCIS codes: (190.2620) Harmonic generation and mixing; (190.4400) Nonlinear optics, materials; (190.4975) Parametric processes.

References and links

1. S. G. Abrahams and J. L. Bernstein, "Luminescent piezoelectric $CdSiP_2$: Normal probability plot analysis, crystal structure, and generalized structure of the $A^{II}B^{IV}C^{V}_2$ family," J. Chem. Phys. **55**(2), 796–803 (1971).
2. G. A. Ambrazyavichyus, G. A. Babonas, and A. Yu. Shileika, "Birefringence of pseudodirect bandgap $A^2B^4C^5_2$ semiconductors," Sov. Phys. Collect. **17**, 51–55 (1977) [transl. from Lit. Fiz. Sb. **17**, 205–211 (1977)].
3. N. Itoh, T. Fujinaga, and T. Nakau, "Birefringence in $CdSiP_2$," Jpn. J. Appl. Phys. **17**(5), 951–952 (1978).
4. E. Buehler and J. H. Wernick, "Concerning growth of single crystals of the II-IV-V diamond-like compounds $ZnSiP_2$, $CdSiP_2$, $ZnGeP_2$, and $CdSnP_2$ and standard enthalpies of formation for $ZnSiP_2$ and $CdSiP_2$," J. Cryst. Growth **8**(4), 324–332 (1971).
5. N. A. Goryunova, L. B. Zlatkin, and K. K. Ivanov, "Optical anisotropy of $A^2B^4C^5_2$ crystals," J. Phys. Chem. Solids **31**(11), 2557–2561 (1970).
6. G. Ambrazyavichyus, G. Babonas, and V. Karpus, "Optical activity of $CdSiP_2$," Sov. Phys. Semicond. **12**, 1210–1211 (1978) [trasl. from Fiz. Tekh. Poluprovodn. **12**, 2034–2036 (1978)].
7. A. Ambrazevicius and G. Babonas, "Dependence of birefringence of pseudodirect gap $A^2B^4C^5_2$ compounds on hydrostatic pressure and on temperature," Sov. Phys. Collect. **18**, 52–59 (1978) [transl. from Lit. Fiz. Sb. **18**, 765–774 (1978)].
8. P. G. Schunemann, K. T. Zawilski, T. M. Pollak, D. E. Zelmon, N. C. Fernelius, and F. Kenneth Hopkins, "New nonlinear optical crystal for mid-IR OPOs: $CdSiP_2$," Advanced Solid-State Photonics, Nara, Japan, Jan. 27–30, 2008, Conference Program and Technical Digest, Post-Deadline Paper MG6.
9. P. G. Schunemann, K. T. Zawilski, T. M. Pollak, V. Petrov, and D. E. Zelmon, "$CdSiP_2$: a new nonlinear optical crystal for 1 and 1.5-micron-pumped, mid-IR generation," Advanced Solid-State Photonics, Denver (CO), USA, Feb. 1–4, 2009, Conference Program and Technical Digest, Paper TuC6.
10. K. T. Zawilski, P. G. Schunemann, T. C. Pollak, D. E. Zelmon, N. C. Fernelius, and F. K. Hopkins, "Growth and characterization of large $CdSiP_2$ single crystals," J. Cryst. Growth **312**(8), 1127–1132 (2010).
11. V. Petrov, F. Noack, I. Tunchev, P. Schunemann, and K. Zawilski, "The nonlinear coefficient d_{36} of $CdSiP_2$," Proc. SPIE **7197**, 71970M (2009).
12. P. D. Mason, D. J. Jackson, and E. K. Gorton, "CO_2 laser frequency doubling in $ZnGeP_2$," Opt. Commun. **110**(1-2), 163–166 (1994).
13. V. Petrov, V. Badikov, and V. Panyutin, "Quaternary nonlinear optical crystals for the mid-infrared spectral range from 5 to 12 micron," in *Mid-Infrared Coherent Sources and Applications*, M. Ebrahim-Zadeh and I. Sorokina, eds., *NATO Science for Peace and Security Series - B: Physics and Biophysics* (Springer, 2008), pp. 105–147.
14. L. P. Gonzalez, D. Upchurch, J. O. Barnes, P. G. Schunemann, K. Zawilski, and S. Guha, "Second harmonic generation in $CdSiP_2$," Proc. SPIE **7197**, 71970N (2009).
15. W. R. L. Lambrecht and X. Jiang, "Noncritically phase-matched second-harmonic-generation chalcopyrites based on $CdSiAs_2$ and $CdSiP_2$," Phys. Rev. B **70**(4), 045204 (2004).
16. G. Ghosh, "Dispersion of temperature coefficients of birefringence in some chalcopyrite crystals," Appl. Opt. **23**(7), 976–978 (1984).

#155014 - $15.00 USD Received 19 Sep 2011; revised 13 Oct 2011; accepted 13 Oct 2011; published 17 Oct 2011

17. P. G. Schunemann, L. A. Pomeranz, K. T. Zawilski, J. Wei, L. P. Gonzalez, S. Guha, and T. M. Pollak, "Efficient mid-infrared optical parametric oscillator based on $CdSiP_2$," Advances in Optical Materials, San Jose (CA), USA, Oct. 14–15, 2009, Conference Program and Technical Digest, Paper AWA3.
18. V. Kemlin, P. Brand, B. Boulanger, P. Segonds, P. G. Schunemann, K. T. Zawilski, B. Ménaert, and J. Debray, "Phase-matching properties and refined Sellmeier equations of the new nonlinear infrared crystal $CdSiP_2$," Opt. Lett. **36**(10), 1800–1802 (2011).
19. K. Kato, N. Umemura, and V. Petrov, "Sellmeier and thermo-optic dispersion formulas for $CdSiP_2$," J. Appl. Phys. **109**(11), 116104 (2011).
20. V. Petrov, G. Marchev, P. G. Schunemann, A. Tyazhev, K. T. Zawilski, and T. M. Pollak, "Subnanosecond, 1 kHz, temperature-tuned, noncritical mid-infrared optical parametric oscillator based on $CdSiP_2$ crystal pumped at 1064 nm," Opt. Lett. **35**(8), 1230–1232 (2010).
21. G. C. Bhar, "Sphalerite vibration mode in chalcopyrites," Phys. Rev. B **18**(4), 1790–1793 (1978).
22. M. Bettini, W. Bauhofer, M. Cardona, and R. Nitsche, "Optical phonons in $CdSiP_2$," Phys. Status Solidi B **63**(2), 641–648 (1974).
23. V. Petrov, M. Ghotbi, O. Kokabee, A. Esteban-Martin, F. Noack, A. Gaydardzhiev, I. Nikolov, P. Tzankov, I. Buchvarov, K. Miyata, A. Majchrowski, I. V. Kityk, F. Rotermund, E. Michalski, and M. Ebrahim-Zadeh, "Femtosecond nonlinear frequency conversion based on BiB_3O_6," Laser Photon. Rev. **4**(1), 53–98 (2010).
24. P. S. Kuo, K. L. Vodopyanov, M. M. Fejer, D. M. Simanovskii, X. Yu, J. S. Harris, D. Bliss, and D. Weyburne, "Optical parametric generation of a mid-infrared continuum in orientation-patterned GaAs," Opt. Lett. **31**(1), 71–73 (2006).
25. A. Birmontas, A. Piskarskas, and A. Stabinis, "Dispersion anomalies of tuning characteristics and spectrum of an optical parametric oscillator," Sov. J. Quantum Electron. **13**(9), 1243–1245 (1983) [transl. from Kvantovaya Elektron. (Moscow) **10**, 1881–1884 (1983)].
26. B. Bareīka, A. Birmontas, G. Dikchyus, A. Piskarskas, V. Sirutkaitis, and A. Stabinis, "Parametric generation of picosecond continuum in near-infrared and visible ranges on the basis of a quadratic nonlinearity," Sov. J. Quantum Electron. **12**(12), 1654–1656 (1982) [transl. from Kvantovaya Elektron. (Moscow) **9**, 2534–2536 (1982)].
27. J.-J. Zondy and D. Touahri, "Updated thermo-optic coefficients of $AgGaS_2$ from temperature-tuned noncritical $3\omega\ \omega \rightarrow 2\omega$ infrared parametric amplification," J. Opt. Soc. Am. B **14**(6), 1331–1338 (1997).
28. D. A. Roberts, "Dispersion equations for nonlinear optical crystals: KDP, $AgGaSe_2$, and $AgGaS_2$," Appl. Opt. **35**(24), 4677–4688 (1996).
29. G. C. Bhar and G. Ghosh, "Temperature-dependent Sellmeier coefficients and coherence lengths for some chalcopyrite crystals," J. Opt. Soc. Am. **69**(5), 730–733 (1979).
30. S. I. Orlov, E. V. Pestryakov, and Y. N. Polivanov, "Optical parametric amplification with a bandwidth exceeding an octave," Quantum Electron. **34**(5), 477–481 (2004) [transl. from Kvantovaya Elektron. (Moscow) **34**, 477–481 (2004)].
31. T. Skauli, P. S. Kuo, K. L. Vodopyanov, T. J. Pinguet, O. Levi, L. A. Eyres, J. S. Harris, M. M. Fejer, B. Gerard, L. Becouarn, and E. Lallier, "Improved dispersion relations for GaAs and applications to nonlinear optics," J. Appl. Phys. **94**(10), 6447–6455 (2003).
32. E. Takaoka and K. Kato, "Thermo-optic dispersion formula for $AgGaS_2$," Appl. Opt. **38**(21), 4577–4580 (1999).
33. E. Tanaka and K. Kato, "Thermo-optic dispersion formula of $AgGaSe_2$ and its practical applications," Appl. Opt. **37**(3), 561–564 (1998).
34. J.-J. Zondy, D. Touahri, and O. Acef, "Absolute value of the d_{36} nonlinear coefficient of $AgGaS_2$: prospect for a low-threshold doubly resonant oscillator-based 3:1 frequency divider," J. Opt. Soc. Am. **14**(10), 2481–2497 (1997).
35. J.-J. Zondy, "Experimental investigation of single and twin $AgGaSe_2$ crystals for CW 10.2 μm SHG," Opt. Commun. **119**(3-4), 320–326 (1995).
36. T. Skauli, K. L. Vodopyanov, T. J. Pinguet, A. Schober, O. Levi, L. A. Eyres, M. M. Fejer, J. S. Harris, B. Gerard, L. Becouarn, E. Lallier, and G. Arisholm, "Measurement of the nonlinear coefficient of orientation-patterned GaAs and demonstration of highly efficient second-harmonic generation," Opt. Lett. **27**(8), 628–630 (2002).

1. Introduction

The nonlinear optical crystal $CdSiP_2$ (CSP) belongs to the tetragonal point group $\bar{4}2m$, with lattice constants a = 5.68Å, c = 10.431 Å, and Z = 4 for the unit cell parameters [1]. It was grown in the past in small sizes that did not allow measurement of essential physical properties [2–7].

CSP is optically negative uniaxial chalcopyrite so that non-critical type-I (oo-e) phase-matching is possible in contrast to the positive $ZnGeP_2$ (ZGP) which is the only commercially available II-IV-V_2 type chalcopyrite. The birefringence, (n_e-n_o), of CSP was found to be - 0.06 approaching a wavelength of 6 μm [2], - 0.051 near 2 μm [7], - 0.05 at 1 μm [5], and - 0.045 at 840 nm [3] in earlier work. An isotropic point, *i.e.* $n_e = n_o$, was also observed close to the

#155014 - $15.00 USD Received 19 Sep 2011; revised 13 Oct 2011; accepted 13 Oct 2011; published 17 Oct 2011

band-edge [5–7]: at room temperature this point occurs at 2.41 eV (514.5 nm) [6,7] and near this point, optical activity can be observed [6].

Recently, high optical quality crystals of CSP with sizes reaching 70 × 25 × 8 mm^3 were grown successfully from the melt by using high purity starting materials via the horizontal gradient freeze technique [8–10]. Important physical characteristics, including transparency, birefringence, and thermo-mechanical properties have already been measured and can be found in the literature [10].

In the present work we analyze the nonlinear and dispersive properties of CSP predicting broadband continuum generation phase-matching at a pump wavelength of 2.43 μm. A comparison with other chalcopyrite materials in the context of super-continuum generation through a second-order nonlinear process is also established.

2. Nonlinearity of CSP

The value of the d_{36} nonlinear optical coefficient of CSP was estimated relative to ZGP by second-harmonic generation (SHG) near 4.6 μm [11]. The fundamental beam that we used was produced by a femtosecond $KNbO_3$-based optical parametric amplifier (OPA) pumped near 800 nm at a repetition rate of 1 kHz. The OPA used a 6-mm-long $KNbO_3$ crystal cut at θ = 41.9° for type I phase matching. As an OPA seed we used the frequency doubled idler output of a BBO type-II OPA near 1 μm. The idler pulses of the $KNbO_3$ OPA were temporally broadened but simultaneously spectrally narrowed (typical FWHM of 90 nm). The uncoated CSP sample was 0.53 mm thick with an aperture of 7 × 7 mm^2. It was cut at (θ = 43°, φ = 45°) for type-I SHG. An uncoated sample of ZGP, cut at (θ = 50.5°, φ = 0°) with identical size and thickness, was used as a reference.

For the chosen wavelength and crystal thickness, the spectral acceptance was much larger than the spectral extent of the pump pulses (~12 times for CSP and ~7 times for ZGP). The angular acceptance was also much larger (>11 times for CSP and >16 times for ZGP) than the angular extent of the incident beam focused by a 25 cm BaF_2 lens. Finally, according to the beam diameter at the position of the crystals, the birefringence walk-off ($\tan\rho$ = 0.009 for CSP and $\tan\rho$ = 0.005 for ZGP) could be neglected. The incident pulse energy near 4.6 μm was limited to less than 2 μJ and the internal conversion efficiency was below 10%. This justifies the plane-wave approximation. The effective nonlinear coefficient was estimated by correcting the relative SHG efficiency only for the different Fresnel losses and index of refraction although both corrections did not exceed 5%.

An average of 20 measurements for each crystal was taken, in which the results in terms of SHG output did not deviate by more than ± 5%. The experimentally measured internal phase-matching angles were used then to derive the ratio for the d_{36} coefficients: we found d_{36}(CSP) = 1.07d_{36}(ZGP) with a relative error estimate of ± 5%. Assuming d_{36} = 75 pm/V for of ZGP at a fundamental wavelength of λ_F = 9.6 μm [12], which gives 79 pm/V at λ_F = 4.56 μm when using Miller's rule, it is found d_{36} = 84.5 pm/V for CSP at λ_F = 4.56 μm.

As a test for the reliability of the measurement, we also measured d_{36} of $HgGa_2S_4$ relative to ZGP using a sample of 0.48 mm thickness cut at (θ = 38.6°, φ = 45°) for type-I SHG. The result was $d_{36}(HgGa_2S_4)$ = 0.328d_{36}(ZGP) at λ_F = 4.58 μm, leading to $d_{36}(HgGa_2S_4)$ = 25.9 pm/V near 4.6 μm, which is in very good agreement with previous estimates using the Maker fringe technique at 1064 nm or SHG at 3.5 μm, *i.e.* $d_{36}(HgGa_2S_4) \approx 1.8 d_{36}(AgGaS_2)$ [13]·.

Fully independent, the result for d_{36}(CSP) was confirmed in frequency doubling of 100 ns long pulses at the second harmonic (λ_F = 4.78 μm) of a TEA CO_2 laser operating at 4 Hz repetition rate [14].

3. Sellmeier equations and phase-matching properties

The different Sellmeier equations that have been proposed in previous works for CSP are listed in Table 1. The first Sellmeier equations that appeared in the literature on CSP were in fact derived from first-principles band structure calculations [15]. Two versions of Sellmeier

#155014 - $15.00 USD Received 19 Sep 2011; revised 13 Oct 2011; accepted 13 Oct 2011; published 17 Oct 2011

equations appeared more recently based on ordinary and extraordinary principal refractive index measurement by the minimum deviation method with a 30° prism in the 0.66 µm - 5 µm wavelength range [8,9]. The latter one predicts an isotropic point at 508.8 nm [9]. In addition, the birefringence was independently derived from polarized light interference spectra in the entire transparency range of CSP [10].

Note that, based on older data of the temperature dependence of the birefringence [7], thermo-optic coefficients had also been fitted for CSP [16]. The Sellmeier coefficients of Schunemann *et al*. [9] were also extended with temperature dependence, with validity between 10°C and 70°C, which was derived fitting optical parametric oscillator (OPO) tuning data recorded for a pump wavelength of 1.99 µm emitted by a Tm:YALO laser [17].

Table 1. Different Sets of Sellmeier Equations for $CdSiP_2$ at Room Temperature Previously Published and Listed by Chronological Order

Sellmeier expressions	References
$n_o^2 = 6.747 + 4.784\ \lambda^2/(\lambda^2-0.076) + 1.5\ \lambda^2/(\lambda^2-420)$ $n_e^2 = 7.107 + 4.107\ \lambda^2/(\lambda^2-0.086) + 1.5\ \lambda^2/(\lambda^2-420)$	[15] (Lambrecht, 2004)
$n_o^2 = 2.931 + 6.4248\ \lambda^2/(\lambda^2-0.1028) - 0.0032818\ \lambda^2$ $n_e^2 = 3.4975 + 5.5451\ \lambda^2/(\lambda^2-0.11713) - 0.0031242\ \lambda^2$	[8] (Schunemann, 2008)
$n_o^2 = 3.0811 + 6.2791\ \lambda^2/(\lambda^2-0.10452) - 0.0034888\ \lambda^2$ $n_e^2 = 3.4343 + 5.6137\ \lambda^2/(\lambda^2-0.11609) - 0.0034264\ \lambda^2$	[9] (Schunemann, 2009)
$n_o^2 = 3.0449 + 1.214 \times 10^{-4}T + (6.1164 + 5.459 \times 10^{-4}\ T)\ \lambda^2/(\lambda^2-0.10452) - 0.0034888\ \lambda^2$ $n_e^2 = 3.3978 + 1.224 \times 10^{-4}T + (5.4297 + 6.174 \times 10^{-4}\ T)\ \lambda^2/(\lambda^2-0.11609) - 0.0034264\ \lambda^2$	[17], T[K] (Schunemann, 2009)
$n_o^2 = 3.72202 + 5.91985\ \lambda^2/(\lambda^2-0.06408) + 3.92371\ \lambda^2/(\lambda^2-2071.59)$ $n_e^2 = 4.68981 + 4.77331\ \lambda^2/(\lambda^2-0.08006) + 0.91879\ \lambda^2/(\lambda^2-496.71)$	[18] (Kemlin, 2011)
$n_o^2 = 11.4442 + 0.65652/(\lambda^2-0.10464) + 1286.198/(\lambda^2-617.005)$ $n_e^2 = 11.3443 + 0.64705/(\lambda^2-0.11803) + 1512.410/(\lambda^2-658.867)$	[19] (Kato, 2011)

These Sellmeier equations were then modified by Kato *et al.* [19] by taking into account the experimental OPO wavelengths for non-critical room-temperature phase-matching at a pump wavelength of 1064.2 nm [20], as well as the introduction of the isotropic point at room temperature. These equations were also extended with thermo-optic coefficients, as it will be shown in the next section, based on the same 1.99 µm pumped OPO tuning data [17] and the non-critical OPO tuning data recorded in the 25°C - 150°C temperature range [20]. The validity of the Sellmeier and thermo-optic coefficients [19] was specified from the isotropic point up to the long-wave clear transparency limit of CSP around 6.5 µm [10]. Finally, the Sellmeier equations of Kemlin *et al.* [18] were determined from independent phase-matching angle measurements between 3 µm and 9.5 µm using the sphere method.

The physical validity of these Sellmeier equations can be assessed from the corresponding infrared pole wavelengths λ_{IR}. These values were taken as initial parameters at $\lambda_{IR}^{o,e} = 20.4$ µm

#155014 - $15.00 USD Received 19 Sep 2011; revised 13 Oct 2011; accepted 13 Oct 2011; published 17 Oct 2011

for both the ordinary and the extraordinary indices by Lambrecht *et al.* in their calculations [15]. The Sellmeier equations of Schunemann *et al.* [8,9,17] cannot provide $\lambda_{IR}^{o,e}$ since the fits were based on expressions using infrared correction terms. In the case of Kemlin *et al.* [18], the values can be deduced from the ordinary and extraordinary refractive index equations that were experimentally obtained, which leads to λ_{IR}^{o} = 45.5 µm and λ_{IR}^{e} = 22.2 µm respectively. The procedure is the same for Kato *et al.* [19], but the two infrared poles obtained are closer, *i.e.* λ_{IR}^{o} = 24.8 µm and λ_{IR}^{e} = 25.6 µm. Note that all these values are compatible with several optically active phonons measurements previously reported [21,22].

Figures 1 and 2 compare the SHG and difference-frequency generation (DFG) phase-matching directions measured by Kemlin *et al.* [18] with those predicted by the other Sellmeier equations from Table 1.

The DFG phase-matching curves predicted by the equations of Lambrecht *et al.* [15] are not shown in Fig. 2 because they noticeably deviate from the experimental points. Nevertheless, the discrepancy is not so large in the case of SHG, which is a good result for dispersion equations coming from a computational method. The best agreement is obtained with the equations of Kemlin *et al*. [18].

The temperature dependence of the Sellmeier equations is an important issue for applications. We then combined the room temperature equations of Kemlin *et al.* [18] with the thermo-optic coefficients derived by Kato *et al.* [19], which provides the following expressions for the ordinary and extraordinary refractive indices of CSP:

$$n_o(\lambda,T)=\begin{cases}\left(3.72202+\dfrac{5.91985\lambda^2}{\lambda^2-0.06408}+\dfrac{3.92371\lambda^2}{\lambda^2-2071.59}\right)^{1/2}\\ +10^{-5}(T-21)\left(\dfrac{1.1538}{\lambda^3}-\dfrac{1.1955}{\lambda^2}+\dfrac{0.7263}{\lambda}+10.8238\right)\end{cases}$$

$$n_e(\lambda,T)=\begin{cases}\left(4.68981+\dfrac{4.77331\lambda^2}{\lambda^2-0.08006}+\dfrac{0.91879\lambda^2}{\lambda^2-496.71}\right)^{1/2}\\ +10^{-5}(T-21)\left(\dfrac{1.3732}{\lambda^3}-\dfrac{0.6361}{\lambda^2}+\dfrac{0.8303}{\lambda}+11.4051\right)\end{cases} \quad (1)$$

The temperature T is expressed in [°C] and the wavelength λ in [µm]. Equations (1) are the temperature-dependent Sellmeier equations of highest accuracy for CSP to the best of our knowledge.

#155014 - $15.00 USD Received 19 Sep 2011; revised 13 Oct 2011; accepted 13 Oct 2011; published 17 Oct 2011

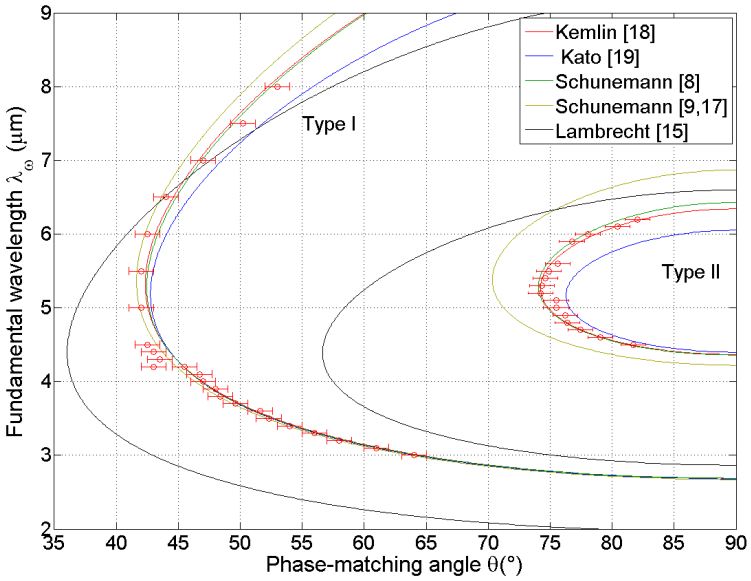

Fig. 1. Type-I SHG ($\lambda_\omega{}^o$, $\lambda_\omega{}^o$, $\lambda_{2\omega}{}^e$) and type-II SHG ($\lambda_\omega{}^o$, $\lambda_\omega{}^e$, $\lambda_{2\omega}{}^e$) tuning curves at 21°C of $CdSiP_2$. The fundamental wavelength λ_ω is given as a function of the phase-matching angle θ. Circles stand for experimental data [18]. (o) and (e) stand for the ordinary and extraordinary polarizations, respectively.

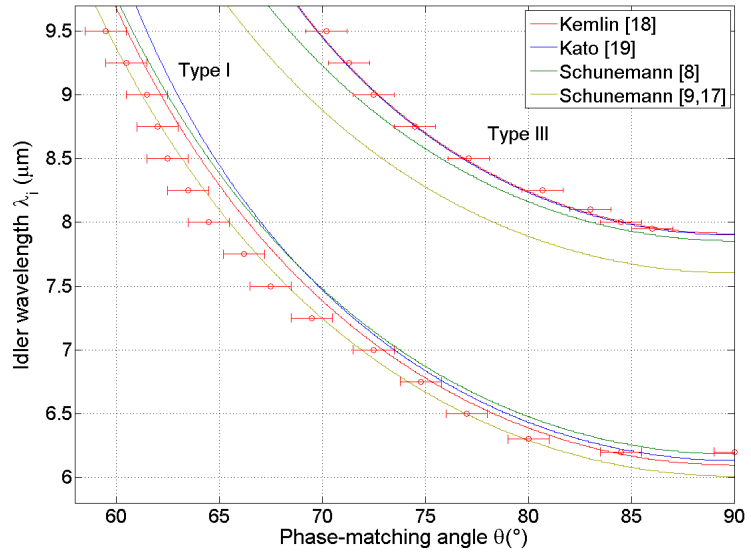

Fig. 2. Type-I DFG ($\lambda_p{}^e$, $\lambda_s{}^o$, $\lambda_i{}^o$) and type-III DFG ($\lambda_p{}^e$, $\lambda_s{}^e$, $\lambda_i{}^o$) angular tuning curves at 21°C of $CdSiP_2$ with a pump at λ_p = 1.064 µm. λ_i stands for the idler wavelength plotted as a function of the phase-matching angle θ. Circles are the experimental data from Kemlin *et al.* [18]. (o) and (e) stand for the ordinary and extraordinary polarizations, respectively.

4. Broadband infrared continuum generation

Continuum generation based on a second-order nonlinear process is attracting recently increasing attention for various applications and the potential to generate such continuum using ultrashort laser pulses has recently been evaluated for a number of oxide materials operating at shorter wavelengths [23]. An OPO where the idler and signal are in the same polarization state is of particular interest for the generation of a broadband continuum.

#155014 - $15.00 USD Received 19 Sep 2011; revised 13 Oct 2011; accepted 13 Oct 2011; published 17 Oct 2011

However, in such OPOs, or for the case of ultrashort pump pulses in the so-called synchronously pumped OPOs, normally only the signal wave is resonated. Thus, to obtain smooth mid-infrared continuum, having in mind that seeding in this spectral range will require additional complexity in the case of OPA, most straightforward of the travelling-wave approaches seems to be the optical parametric generator (OPG), pumped by amplified picosecond or femtosecond pulses that possess sufficient intensity to initiate the parametric process from fluorescence noise [24].

In all the above cases, the nonlinear processes are equivalent to type-I DFG. The spectral acceptance for such DFG is very broad when the first derivative of the angular tuning curve with respect to the wavelength is infinite at degeneracy, *i.e.* at $\lambda_s = \lambda_i = \lambda_p/2$, which leads to a spectrally non-critical phase-matching at the corresponding angle and higher derivatives have to be considered [23]. But phase-matching at degeneracy is not necessarily given at any pump wavelength, as can be seen *e.g.* in Fig. 2 for the case of CSP which is a crystal possessing moderate birefringence at λ_p = 1.064 µm. It is then important to define the pump wavelength range over which an OPO or OPG can be phase-matched at degeneracy.

Furthermore, degenerate phase-matching can be allowed at a pump wavelength λ_p^{Opt} for which the first derivative of the group velocity of the signal and idler waves is vanishing, leading to the broadest wavelength range that can be generated for a given crystal cut at the proper phase-matching angle θ^{Opt} [25]. Experimentally this situation has been realized for the first time in the visible and near-infrared with a picosecond OPG based on KDP [26].

According to Eqs. (1) at 21°C, the above condition is fulfilled in a CSP crystal cut at θ^{Opt} = 42.8° and pumped at λ_p^{Opt} = 2.43 µm. This deviates from an earlier prediction of 2.55 µm [8,9], but it confirms that such wavelengths can be provided from Cr^{2+}:ZnSe or similar laser systems. We performed the same kind of calculation for the commercially available nonlinear chalcopyrite crystals $AgGaS_2$, $AgGaSe_2$ and ZGP using the corresponding Sellmeier equations [27–29], and we found for their respective optimum pump wavelengths λ_p^{Opt} : 2.04 µm, 2.86 µm and 2.63 µm, slightly deviating from the values that can be found in the literature [30]. The corresponding calculated angular tuning curves are plotted in Fig. 3, which shows the complementary of these materials for the generation of mid-infrared super-continuum.

The full wavelength range of the super-continuum emitted by a crystal cut at the phase-matching angle θ^{Opt} can be then estimated from the third derivative of the group velocity [23,25]. While Fig. 3 provides a nice illustration basically valid for DFG, in the case of high parametric gain in an OPG this factor also enters the expression for the bandwidth and the parameter that can be quantitatively compared is the so-called parametric gain bandwidth. Expressed using the FWHM convention, this parametric gain bandwidth is written in the degenerate case [23]:

$$\Delta\nu^{Opt} = \frac{1}{\pi}\left(\frac{\ln 2\Gamma}{L}\right)^{1/8}\left|\frac{24}{\beta_{i,s}}\right|^{1/4} \qquad (2)$$

where the gain factor is defined by $\Gamma^2 = \frac{2\pi^2 d_{eff}^2 I_p}{n_p n_{s,i}^2 \lambda_p^2 \varepsilon_0 c}$, and $1/\beta_{i,s} = \partial^4\omega_{i,s}/\partial k_{i,s}^4$ is the third derivative of the group velocity at λ_p^{Opt} with $k_{i,s}$ denoting the wave vector of the signal or idler waves and $\omega_{i,s}$ denoting the corresponding circular frequencies. I_p is the pump intensity, d_{eff} is the effective nonlinearity, L is the crystal length and $n_{p,s,i}$ denote the refractive indices of the pump, signal and idler waves respectively.

#155014 - $15.00 USD Received 19 Sep 2011; revised 13 Oct 2011; accepted 13 Oct 2011; published 17 Oct 2011

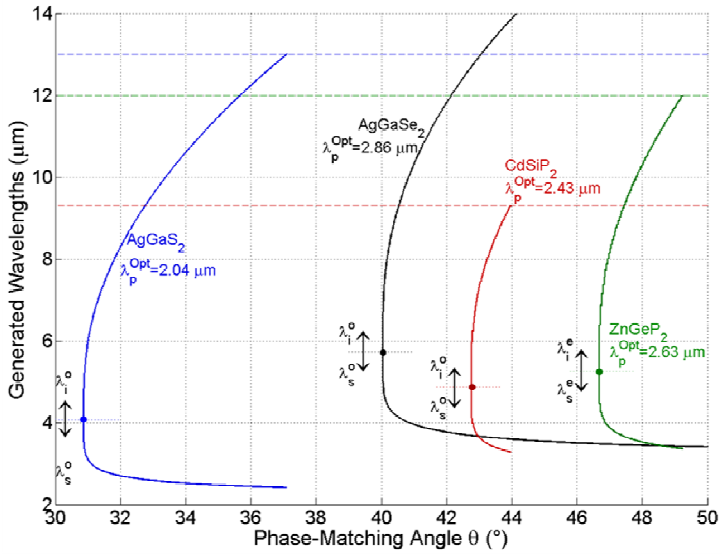

Fig. 3. OPO/OPG angular tuning curves at 21°C of several mid-infrared crystals pumped at the wavelength λ_p^{Opt} corresponding to the broadest range of emission of the signal (λ_s) and idler (λ_i). Except for $AgGaSe_2$, for which the infrared cut-off wavelength is above 14 µm, the tuning ranges of the different materials are determined by the idler mid-infrared absorption limit taken here at $\alpha = 2$ cm^{-1}. The dots correspond to degeneracy, which delimitates the idler range in the upper half-plane and the signal range in the lower half-plane. The indices (o) and (e) denote the ordinary and extraordinary polarizations, respectively.

The values calculated from Eq. (2) are listed in Table 2 for CSP, $AgGaS_2$, $AgGaSe_2$ and ZGP. For comparison, we have assumed a crystal length of $L = 1$ cm and $I_p = 1$ GW/cm^2. In order to complete the comparison, we calculated the broadest continuum that can be generated using a quasi-phase-matched (QPM) orientation-patterned GaAs (OP-GaAs) crystal [31]. Instead of optimum phase-matching angle, there is optimum grating period in this case which amounts to 173 µm. Note that there is a fundamental difference with respect to super-continuum generation when dealing with QPM materials. It is related to the group walk-off of the generated waves with respect to the pump which limits the effective interaction length and hence the conversion efficiency [23]. This fact reflects the plane-wave approximation used to derive Eq. (2), *i.e.* the limited validity of this formalism for ultrashort laser pulses. In order to enable a fair comparison, we selected crystal length and pump intensity that correspond to picosecond rather than femtosecond pump sources, so that the full crystal length can be utilized in the process of parametric amplification. In Table 2 are also given the effective nonlinear coefficients d_{eff} of the different materials in the direction corresponding to θ^{Opt}. For their calculation, we used d_{36} values from the cited literature corrected by Miller's rule for the actual three-wave process. Note that the effective nonlinear coefficient of $AgGaSe_2$, CSP and $AgGaS_2$ is maximum at an azimuthal angle of $\varphi = 45°$, whereas it is maximum at $\varphi = 0°$ for ZGP. Both cases correspond to negative and positive chalcopyrite crystals in type-I phase-matching configuration. The parametric gain bandwidths are not very different for the materials considered due to the weak dependence on the dispersion and even weaker on the gain in Eq. (2). OP-GaAs shows somewhat narrower bandwidth due to the higher $\beta_{i,s}$ value.

The capability to generate a stable broadband super-continuum is closely related to the thermal properties of the nonlinear material. On the basis of the thermo-optic coefficients that are available for the four chalcopyrites [29,32,33] and GaAs [31] under investigation, we calculated the temperature dependence of the $sinc^2(\Delta k(T)L/2)$ function as shown in Fig. 4, and the corresponding thermal acceptances $L.\Delta T$ (FWHM) are included in Table 2.

#155014 - $15.00 USD Received 19 Sep 2011; revised 13 Oct 2011; accepted 13 Oct 2011; published 17 Oct 2011

Table 2. Broadband Continuum Type-I Phase-Matching Parameters for the Four Birefringent Chalcopyrite Crystals Considered and OP-GaAs

Crystals	λ_p^{Opt} [μm]	θ^{Opt} [°]	d_{36}/d_{eff} [pm/V]	Γ [cm^{-1}]	$\beta_{s,i}$ [10^{-54} s/m]	$\Delta\nu^{Opt}$ [THz]	$L\Delta T$ [cm.°C]
$AgGaS_2$	2.04	30.9	13.1/6.7	2.402	9.7 [27,34]	42.5	66 [32]
$CdSiP_2$	2.43	42.8	84.1/57.2	12.04	18 [this work]	44.6	328 [this work]
$ZnGeP_2$	2.63	46.7	77.8/77.6	14.50	37 [12,29]	38.1	484 [29]
$AgGaSe_2$	2.86	40.0	31.0/19.9	4.493	6.5 [28,35]	50.9	>700 [33]
OP-GaAs	3.29	Λ = 173 μm	91/57.9	7.985	130 [31,36]	25.8	66 [31]

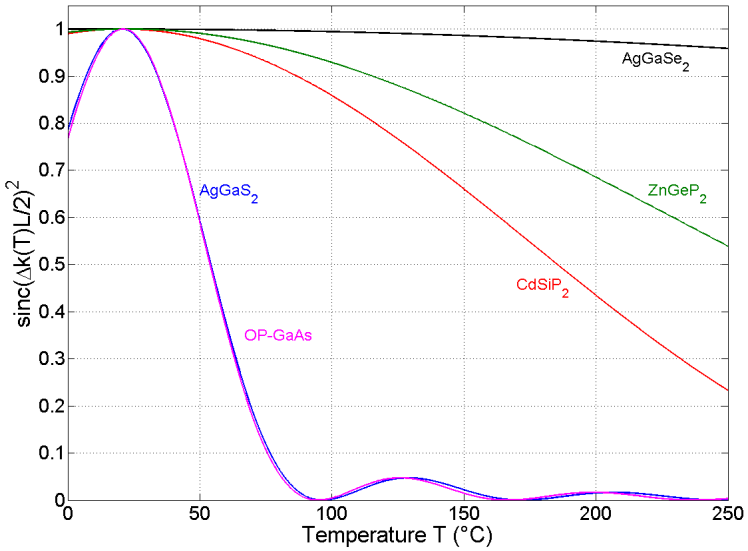

Fig. 4. Calculated temperature dependence of the DFG efficiency in the low conversion limit obtained by the four birefringent chalcopyrite crystals considered and OP-GaAs for the same parameters as in Table 2, assuming a crystal length of L = 1 cm.

The temperature acceptance of CSP is very large but lower than in ZGP. It is known that temperature tuning in ZGP is impractical, contrary to the case of CSP for which this still seems a feasible approach to tune the wavelength [17], also under non-critical phase-matching conditions [20].

5. Conclusion

In conclusion, we compared existing dispersion relations for the CSP nonlinear crystal and extended the most reliable of them with temperature dependence. With the measured nonlinear coefficient, it was possible to estimate the parametric gain bandwidth for the special phase-matching configuration ensuring ultra-broad parametric amplification bandwidth in an OPG pumped by ultrashort pulses. CSP can be pumped by Cr^{2+}:ZnSe ultrafast laser systems or tandem OPGs to generate super-continuum in the mid-infrared extending up to its upper transparency limit.

#155014 - $15.00 USD Received 19 Sep 2011; revised 13 Oct 2011; accepted 13 Oct 2011; published 17 Oct 2011